Talanta 219 (2020) 121211

Contents lists available at ScienceDirect

Talanta

journal homepage: www.elsevier.com/locate/talanta

Homogeneous detection of 5-hydroxymethylcytosine based on electrochemiluminescence quenching of g-C_3N_4/MoS_2 nanosheets by ferrocenedicarboxylic acid polymer

Chengji Sui[1], Qian Wang[1], Yunlei Zhou**, Dingding Zhang, Huanshun Yin*, Shiyun Ai

College of Chemistry and Material Science, Food Safety Analysis and Test Engineering Technology Research Center of Shandong Province, Shandong Agricultural University, 271018, Taian, Shandong, People's Republic of China

ARTICLE INFO

Keywords:
5-Hydroxymethylcytosine
Electrochemiluminescence biosensor
HhaI methyltransferase
Ferrocenedicarboxylic acid polymer
Chicken embryo fibroblast cell
Rice seedling

ABSTRACT

A sensitively homogeneous electrochemiluminescence (ECL) method was developed for 5-hydroxymethylcytosine (5hmC) detection using TiO_2/MoS_2/g-C_3N_4/GCE as substrate electrode, where g-C_3N_4 was employed as the ECL active material, the MoS_2 nanosheets were used as co-catalyst, and TiO_2 was adopted as phosphate group capture reagent. To achieve the specific recognition and capture of 5hmC, the covalent reaction between –CH_2OH and –SH was employed under the catalysis of HhaI methyltransferase, in which, –SH functionalized ferrocenedicarboxylic acid polymer (PFc-SH) was prepared as 5hmC capture reagent and ECL signal quencher. Then, based on the interaction between TiO_2 and phosphate group of 5hmC, the target was recognized and captured on electrode, resulting in a decreased ECL response due to the quenching effect of PFc-SH. Under optimal conditions, the biosensor presented the linear range from 0.01 to 500 nM with the detection limit of 3.21 pM (S/N = 3). The steric effect on electrode surface is a bottle-neck issue restricting devised biosensors advancement. In this work, the reaction between 5hmC and PFc was carried out in the solution, which can avoid steric effect on electrode surface to keep the high activity of enzyme. In addition, the biosensor was successfully applied to detect 5hmC in genomic DNA of chicken embryo fibroblast cells and different tissues of rice seedlings.

1. Introduction

5-Hydroxymethylcytosine (5hmC) is the oxidation product of 5-methylcytosine (5mC), which was first found in 1952 in virus [1]. Unfortunately, it did not attract the attention of researchers at that time. Until 5hmC was found in the nucleotides of Purkinje cells (0.6%) and granule cells (0.2%), more scientists are committed to investigate the biological function of 5hmC [2]. Because of the important role in regulations of gene activity, nuclear reprogramming, and initiation of DNA demethylation in mammals, 5hmC is considered as the sixth deoxyribonucleic acid base [3]. In addition, the content of 5hmC decreases strongly in some cancer cells, including brain, liver, kidney and breast [4], which demonstrates that 5hmC may be an indicator for some cancer diagnosis. In addition, aberrant 5hmC content has also been found in myelodysplastic syndrome, Alzheimer's disease, psychosis, and Huntington's disease [5]. Therefore, 5hmC detection is of great significance. Recently, more and more nano technology has been applied in detection of drugs [6,7].

Up to now, various methods have been developed for 5hmC detection, including capillary electrophoresis-electrospray ionization–mass spectrometry, thin layer chromatography, general bisulfite sequencing, liquid chromatography assembled with tandem mass spectrometry, single-molecule real-time sequencing, fluorescence, electrochemistry, photoelectrochemistry and electrochemiluminescence (ECL) [8–14]. Among them, ECL technique has attracted more attentions in the analytical field due to the advantages of low cost, rapid response, low background signal and high sensitivity.

ECL is a new analytical technique, which combines the advantages of potential controllability of electrochemistry and high sensitivity of chemiluminescence. By applying a certain voltage to carry out electrochemical reaction, electrical biomass is generated on the surface of the electrode, and then these substances are transmitted electronically with themselves or other components in the system to convert into an excited state. At the end, the excited state converts to the ground state,

* Corresponding author.
** Corresponding author.
E-mail addresses: zhyl@sdau.edu.cn (Y. Zhou), yinhs@sdau.edu.cn (H. Yin).
[1] Chengji Sui and Qian Wang contributed equal to this work.

https://doi.org/10.1016/j.talanta.2020.121211
Received 10 February 2020; Received in revised form 18 May 2020; Accepted 21 May 2020
Available online 28 May 2020
0039-9140/ © 2020 Elsevier B.V. All rights reserved.

accompanied by luminescence in the process [15]. It has been widely applied to detect various targets, including alpha fetoprotein [16], histone acetyltransferase [17], carcinoembryonic antigen [18], antibiotics [19,20], ATP [21], DNA [22], microRNA [23,24], 5hmC [25,26] and cell [27,28]. Therefore, the ECL technique was employed to detect 5hmC in this work.

The differentiating between 5mC and 5hmC is difficult due to similarities in their structures. Although the 5hmC antibody has been applied to distinguish 5hmC, there are some problems, such as false positive, expensive price, and large differences between batches. To solve these problems, the researchers found that some special covalent reactions of $–CH_2OH$ on 5hmC can differentiate 5hmC from 5mC. For example, Li et al. presented an approach, which uses specific oxidation of $–CH_2OH$ on 5hmC to produce the –CHO by $KRuO_4$ to achieve the sensitive detection of 5hmC [11]. Song et al. selected T4 β-glucosyltransferase as the specific recognition unit to transfer a glycosyl to the hydroxyl group of 5hmC [29]. Liutkevičiūtė et al. used the reaction between $–CH_2OH$ of 5hmC and thiol compounds catalyzed by HhaI methyltransferase (M. HhaI) to differentiate 5hmC from 5mC [30]. By these reactions, some active molecules can be captured on the 5hmC, which can specially recognize and capture 5hmC by further reaction of the active molecules. Moreover, those methods based on the reaction of $–CH_2OH$ can prove the effective discrimination of 5hmC from 5mC due to the absence of $–CH_2OH$ group on 5mC.

Inspired by the specific covalent reaction between $–CH_2OH$ and thiol compounds catalyzed by M. HhaI, a sensitive ECL biosensor was developed for the detection of 5hmC. More importantly, the reaction between 5hmC and PFc was carried out in the solution, which can better keep the activity of M. HhaI to ensure that the reaction is fully carried out [31,32]. The biosensor possesses excellent stability, sensitivity and reproducibility. Moreover, the 5hmC level in genomic DNA of rice seedling after treated with different antibiotics and chicken embryo fibroblast cell after infected with MDV was investigated by this biosensor, indicating the practicality of the biosensor.

2. Experimental section

2.1. Reagents and apparatus

Thiourea, ammonium molybdate, titanium butoxide, cysteamine hydrochloride, N-hydroxysuccinimide (NHS), N-(3-dimethylaminopropyl)-N-ethyl carbodiimide hydrochloride (EDC), sodium borohydride ($NaBH_4$) and melamine were provided by Aladdin (Shanghai, China). Ferrocenedicarboxylic acid was purchased from Macklin Biochemical Co., Ltd. (Shanghai, China). 2′-Deoxycytidine-5′-triphosphate(dCTP), 2′-deoxythymidine-5′-triphosphate(dTTP), 2′-deoxyguanosine-5′-triphosphate(dGTP) and 2′-deoxyadenosine-5′-triphosphate (dATP) were obtained from Sangon Biotech (Shanghai). N6-methyl-2′-adenosine-5′-triphosphate (m6-ATP), 5-methyl-2′-deoxycytidine-5′-triphosphate (5 m-dCTP) and 5-hydroxymethyl-2′-deoxycytidine-5′-triphosphate (5hm-dCTP) were ordered from Trilink BioTechnologies (San Diego, USA). Rice seeds were bought from a local market. Chicken embryo fibroblast cell after being infected with Marek's disease virus (MDV) were provided by College of Animal and Technology, Shandong Agricultural University. HhaI methyltransferase was bought from NEB (USA). Buffer solutions used in this work were as follows. M. HhaI reaction buffer, 50 mM Tris-HCl (pH 7.4), 10 mM EDTA. Wash buffer, 10 mM Tris-HCl (pH 7.4). Detection buffer, 100 mM $K_2S_2O_8$, 10 mM Tris-HCl (pH 7.4).

Transmission electron microscopy (TEM) was given by Tecnai G2 20 (FEI, USA). X-Ray diffractometer equipment (XRD) was obtained from Smartlab SE (Rigaku, Japan). Scanning electron microscope (SEM) and energy dispersive spectroscopy (EDS) were carried out on a QUANTA250 (FEI, USA). Fourier transform infrared spectra (FT-IR) were detected on a Thermo Nicolet-380 IR spectrophotometer (USA). Electrochemical impedance spectroscopy (EIS) was got from CHI660C electrochemical workstation (CH instruments, Austin, USA). The ECL intensities were measured by MPI-E multifunctional electrochemical and chemiluminescence analytical system (Xi'an Remax Analytical Instrument Ltd. Co. China), with an ECL analyzer between −1.5 and 0 V at 100 mV s^{-1} in 8 mL of detection buffer.

2.2. Preparation of g-C_3N_4 nanosheets

The g-C_3N_4 was prepared by high temperature calcination [33]. The process was described in Supplementary Materials, and the reaction for preparation of g-C_3N_4 was described as Fig. S1.

2.3. Preparation of MoS_2 nanosheets

MoS_2 nanosheets were prepared by the typical hydrothermal method [34]. 64.5 mmol thiourea and 2.2 mmol ammonium molybdate were added into 75 mL double distilled water under strong stirring to form a homogeneous solution. Then, the solution was transferred into a Teflon-lines stainless steel autoclave and heated at 180 °C for 24 h. After cooling naturally to room temperature, the product was washed with double distilled water and ethanol several times by centrifugation. Finally, the product was dried at 60 °C and ground into a powder for further use.

2.4. Preparation of TiO_2 nanosphere

The TiO_2 was obtained by the previous report and with a few modifications [35]. Firstly, 75 mL ethanol and 75 mL acetonitrile were added into beaker and stirred to form a homogeneous solution. After that, 0.38 mL ammonia (28%) and 0.91 mL deionized water were added into the solution under stirring. Then, 3 mL titanium butoxide was added into the solution and stirred for 6 h. Subsequently, the product was washed with deionized water and ethanol several times and dried at 60 °C. In the end, the TiO_2 was obtained by calcination at 500 °C for 2 h under an N_2 atmosphere.

2.5. Preparation of sulfydryl functionalized ferrocenedicarboxylic acid polymer (PFc)

The PFc was got by the previous report [36]. Firstly, 200 mg ferrocenedicarboxylic acid was dissolved in 200 mL methanol to form an orange solution. To obtain the precipitate, the solution was stirred for 2 h under sunshine with the color of the solution changing from orange to taupe. Next, the product was washed with methanol several times by centrifugation and dried at 60 °C. Afterward, 200 mg product was dispersed into 10 mL deionized water by ultrasound. Subsequently, 4 mL of 100 mM EDC and 2 mL of 100 mM NHS were added into the solution and kept for 2 h under stirring. Afterward, 4 mL of 0.1 M cysteamine hydrochloride was added into the solution and stirred overnight. Finally, the product was washed with deionized water several times and dried at 60 °C for further use.

2.6. Preparation of the biosensor

Firstly, 10 mg g-C_3N_4, 0.5 mg MoS_2 and 5 mg TiO_2 powder were respectively dispersed into 5 mL double-distilled deionized water with the aid of 30 min ultrasonication to obtain the dispersion. Then, the glassy carbon electrode (GCE) was polished to a mirror-like surface by the 30 nm Al_2O_3 slurry following by washing ultrasonically with ethanol and deionized water for 10 min. Subsequently, 20 μL of 2 mg/mL g-C_3N_4 suspension, 0.1 mg/mL MoS_2 suspension, 1 mg/mL TiO_2 suspension were dropped successively on the surface of electrode. After each modification, the electrode was dried under the irradiation of an infrared lamp. The prepared electrodes were named as g-C_3N_4/GCE, MoS_2/g-C_3N_4/GCE, and TiO_2/MoS_2/g-C_3N_4/GCE, respectively. Afterward, 10 μL of M. HhaI reaction buffer containing 100 unit/mL M.

HhaI and 10 μL of different concentration of 5hmC were added into 20 μL of 2 mg/mL PFc suspension and kept at 37 °C for 105 min under shaking. Subsequently, the prepared 5hmC-PFc was washed by washing buffer and re-dispersed in 20 μL deionized water. Thereafter, 20 μL of 5hmC-PFc dispersion was dropped onto the surface of the $TiO_2/MoS_2/g\text{-}C_3N_4$/GCE, and the electrode was incubated in a humid chamber at 37 °C for 90 min. Finally, the electrode (5hmC-PFc/$TiO_2/MoS_2/g\text{-}C_3N_4$/GCE) was washed with washing buffer and the ECL signal was measured on the MPI-E multifunctional electrochemical and chemiluminescence analytical system.

2.7. Real sample preparation

To confirm the application of the biosensor, the 5hmC content in genomic DNA of rice seedling treated with different antibiotics was detected by this biosensor. The processing steps are as follows. Firstly, the rice seeds were sterilized with 2% sodium hypochlorite solution. After that, the rice seeds were washed with sterilized water several times and soaked with sterilized water overnight. Then the rice seeds were cultivated in 25 °C environment with successive light on and off cycles every 12 h. When the high of the rice seedling rise to 12 cm, the rice seedling was treated with100 mL solution containing 100 mg/mL different antibiotic for another 4 days. Next, the leaf, stem and root of the rice seedling was harvested and ground into power with the aid of liquid nitrogen freezing. Subsequently, the genomic DNA was extracted using Plant Genomic DNA Extraction Kit (TianGen, Beijing, China) and concentration of the genomic DNA was detected by Quawell Q3000 micro-volume UV spectrophotometer (USA). Finally, the genomic DNA was dilute to the same concentration and degraded to individual nucleotide components using DNA Degradase™ (Zymo Research, USA).

In addition, the 5hmC level in genomic DNA of chicken embryo fibroblast cell infected with Marek s disease virus (MDV) was also detected. Initially, DF-1 cells were seeded in a 6-well-plate at 200 k cells per well, after cultured for 12 h, cells were treated by virus CVI988 and RMD5 at the concentration of 10^6 PFU/mL per well. Every treatment was repeated three times. And then all DF-1cells proceed to culture at cell incubator. Ultimately, cells were respectively harvested at 24 h, 48 h, and 72 h. Afterword, the genomic DNA was extracted by Animal Genomic DNA Extraction Kit (TianGen, Beijing, China) and treated as above.

3. Results and discussion

3.1. Detection strategy

In this work, a novel and sensitive ECL method was developed for 5hmC detection based on the covalent reaction between –CH_2OH and –SH under the catalysis of M. HhaI and the PFc inhibition of the g-C_3N_4 ECL signal. The biosensor construct process and the detection strategy were shown in Scheme 1. Firstly, $TiO_2/MoS_2/g\text{-}C_3N_4$/GCE was prepared as matrix electrode, where g-C_3N_4 was used as the ECL active material, MoS_2 was selected as co-catalyst [37–39], and the TiO_2 was employed as phosphate recognition reagent. To improve the sensitivity and reproducibility, homogeneous detection strategy was employed. Firstly, sulfydryl functionalized ferrocenedicarboxylic acid polymer (PFc) was synthesized with spherical structure, which was employed as 5hmC recognition and capture reagent by using the covalent chemical reaction between –CH_2OH and –SH under the catalysis effect of M. HhaI. For the production of the compound of 5-hydroxymethyl-2′-deoxycytidine-5′-triphosphate and sulfydryl functionalized ferrocenedicarboxylic acid polymer (5hmC-PFc), the phosphate group of 5hmC is away from the PFc surface, which allows the convenient capture of 5hmC-PFc to the $TiO_2/MoS_2/g\text{-}C_3N_4$/GCE surface based on the specific interaction between TiO_2 and phosphate group. The recognition and capture of 5hmC was performed in solution. It can guarantee the high bioactivity of M. HhaI, which can further ensure the high reaction efficiency between –CH_2OH and –SH and avoid the steric-resistance effect caused by the modified nanomaterial on electrode surface [40]. Finally, based on the quenching effect of PFC on g-C_3N_4 ECL signal, 5hmC can be detected.

3.2. Characterization of materials

The g-C_3N_4 nanosheets were characterized by TEM and XRD. TEM shows that the g-C_3N_4 possesses a characteristic layered structure (Fig. 1A). As shown in Fig. 1B, the peak at 13.12° and 27.6° are indexed to the (100) plane and (002) plane, indicating the successful synthesis of g-C_3N_4. Similarly, the MoS_2 nanosheets were characterized by TEM, SEM and XRD. The TEM and SEM prove the nanosheets morphology of the MoS_2 (Fig. 1C, Fig. S2). Fig. 1D shows the XRD pattern for MoS_2. All the peaks of the sample are indexed to MoS_2 (PDF#75-1539), indicating the successful preparation of MoS_2. TiO_2 was characterized by SEM and XRD. The SEM demonstrates the nanospheres morphology of TiO_2 (Fig. 1E). We can see from Fig. 1F, all the diffraction peaks in the XRD pattern of the sample are indexed to TiO_2 (PDF#84-1285), which confirms the successful synthesis of TiO_2. The morphologies of the PFc was also characterized by TEM. As seen in Fig. 1G, the PFc possesses a characteristic nanosphere structure. To testify the successful modification of sulfydryl on PFc, the FT-IR and EDS of PFc were measured. As shown in Fig. S3, compared with PFc, the FT-IR spectra of PFc treated with cysteamine hydrochloride appears new peak at ~1294, ~1684, ~2530 cm^{-1} (curve b), which are ascribed to C–N stretching vibrations, N–H deformation vibration, S–H stretching vibrations, respectively [41]. Fig. S4 and Fig. 1H show the EDS of PFc and sulfydryl functionalized PFc. The results show that the N, S appear in the sulfydryl functionalized PFc. These results confirm the existence of –SH in the sulfydryl functionalized PFc.

3.3. EIS and ECL characterization of the biosensor

To verify the successful construct of the biosensor, the process of the biosensor was characterized by the EIS. As shown in Fig. 2A, the bare GCE shows a small semicircle in the high frequency region with the electron transfer impedance (R_{et}) of 270 Ω (curve a). After modifying with the g-C_3N_4, the R_{et} increases due to the poor conductivity of the g-C_3N_4 (curve b). When the MoS_2 nanosheets were immobilized on the electrode surface, the R_{et} decreases (curve c). It can be attributed to the fact that the introduction of MoS_2 accelerates electron transfer of the probe on the electrode [42]. When TiO_2 coating on the surface of the electrode, the R_{et} increases, which can be explained by the poor electron transfer capacity of TiO_2 (curve d). In the end, the R_{et} increases strongly when the 5hmC-PFc is captured on the electrode surface due to the spatial structure and insulation property of the 5hmC-PFc (curve e). Those results demonstrate that each step of the biosensor is constructed successfully.

For proving the feasibility of the ECL biosensor, the ECL intensities of different electrode were detected and compared. As shown in Fig. 2B, the g-C_3N_4/GCE shows a strong ECL intensity, indicating the outstanding ECL performance of g-C_3N_4 (curve a). When MoS_2 nanosheets are coated on g-C_3N_4/GCE surface, the ECL intensity increases due to the co-catalysis of MoS_2 (curve b). The compare of ECL intensity between $MoS_2/g\text{-}C_3N_4$/GCE and g-C_3N_4/GCE were made in the Fig. S5. After TiO_2 immobilization, the ECL intensity decreases (curve c). Finally, the ECL intensity decreases significantly when the 5hmC-PFc is captured on the electrode surface, which can be attributed to the ECL quenching effect caused by PFc (curve d). To confirm the key role of the 5hmC in PFc capture, some control experiments were performed. The $TiO_2/MoS_2/g\text{-}C_3N_4$/GCE was incubated with PFc without 5hmC and the ECL intensity of the electrode was then measured. Compared to the ECL intensity of the 5hmC-PFc/$TiO_2/MoS_2/g\text{-}C_3N_4$/GCE, the ECL intensity of the electrode ($TiO_2/MoS_2/g\text{-}C_3N_4$/GCE incubated with PFc) is strongly higher (curve e). The result proves that the PFc cannot be

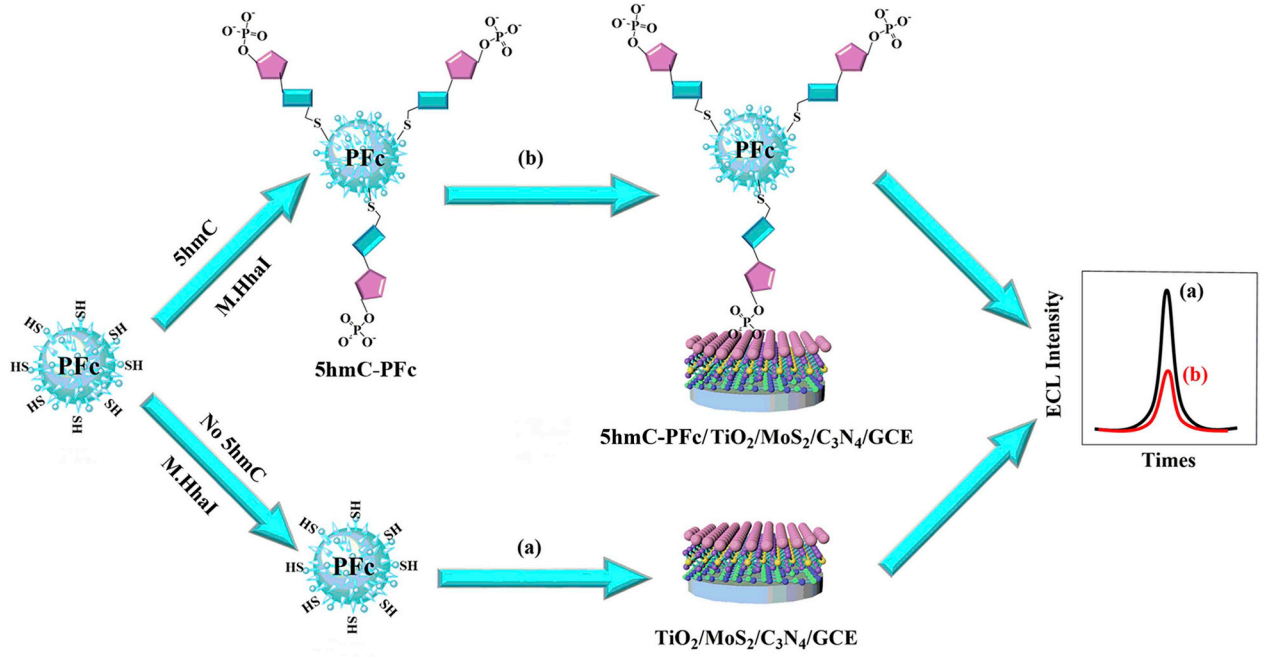

Scheme 1. Schematic illustration of the ECL biosensor fabrication process and 5hmC detection.

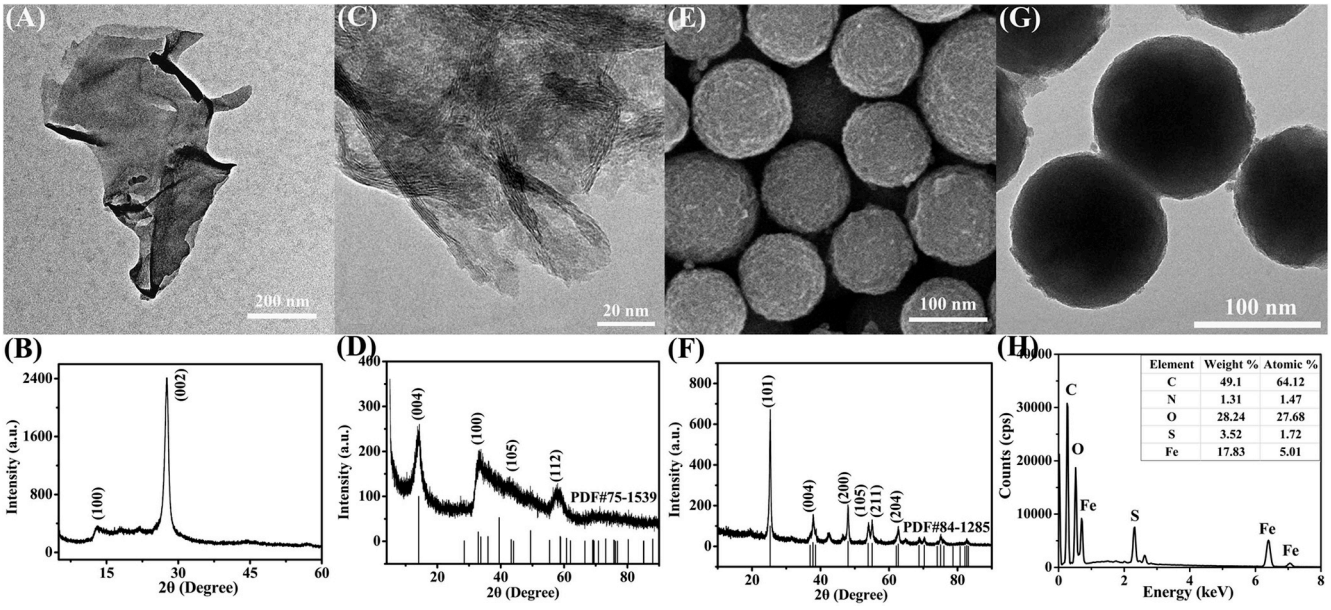

Fig. 1. (A) TEM images of g-C_3N_4, (B) XRD patterns of g-C_3N_4, (C) TEM images of MoS_2, (D) XRD patterns of MoS_2, (E) SEM images of TiO_2, (F) XRD patterns of TiO_2, (G) TEM images of PFc, (H) EDS pattern of sulfydryl functionalized PFc.

captured on the surface of electrode without the 5hmC. After that, the ECL intensity of $TiO_2/MoS_2/g\text{-}C_3N_4$/GCE with 5hmC was measured (curve f). The introduce of 5hmC can cause a slight drop in the ECL intensity of $TiO_2/MoS_2/g\text{-}C_3N_4$/GCE, which can be explained that the formation of less conductive layers on the electrode surface [43]. However, the ECL intensity of $TiO_2/MoS_2/g\text{-}C_3N_4$/GCE with 5hmC was strong higher than that of 5hmC-PFc/$TiO_2/MoS_2/g\text{-}C_3N_4$/GCE. Based on the above analysis, the biosensor can be applied for 5hmC detection by comparing the ECL intensities of different electrode.

3.4. Detection performances of the biosensor for 5hmC detection

To evaluate the detection performance of the biosensor for 5hmC, the ECL intensity of the biosensor fabricated with different concentrations of 5hmC was measured and compared, under the optimized experimental conditions (Figs. S6 and S7, see Supplementary Materials). As shown in Fig. 3A, the ECL intensity decreases with the increase of the 5hmC concentration from 0.01 to 500 nM. In this range, the ECL intensity and the logarithm value of 5hm-dCTP concentration had a linear relationship with the linear regression equation of $I_{ECL} = -1849\log c$ (nM) + 8795 ($R = 0.9950$, Fig. 3B). The detection limit of the biosensor was 3.21 pM (S/N = 3). The detection performances were compared with previous reports and the results were shown in Table 1. The results showed that our biosensor has rational linear range and low detection limit. In addition, from most of the previous works, the researchers mainly focused on the detection of 5hmC in DNA sequence. The main aim of this work is to detect single 5hmC, which is one of the advantages of our work.

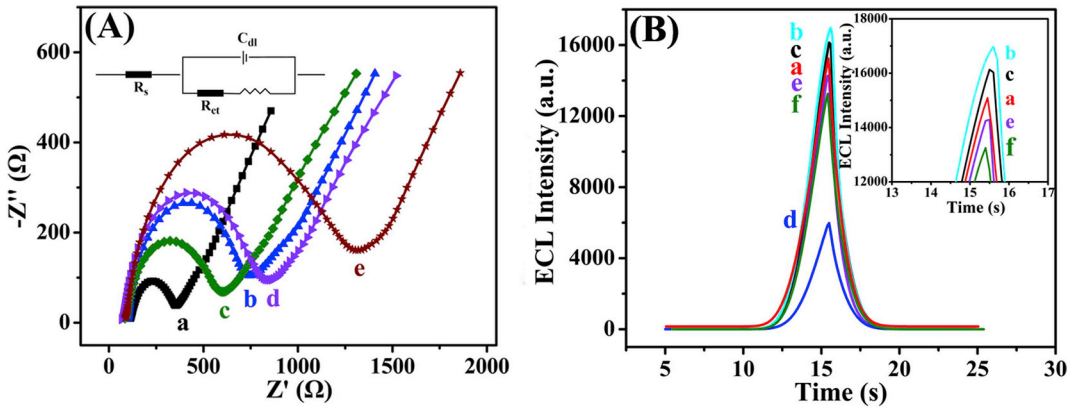

Fig. 2. (A) EIS of (a) GCE, (b) g-C_3N_4/GCE, (c) MoS_2/g-C_3N_4/GCE, (d) TiO_2/MoS_2/g-C_3N_4/GCE, (e) 5hmC-PFc/TiO_2/MoS_2/g-C_3N_4/GCE in 5 mM $K_3[Fe(CN)_6]$/$K_4[Fe(CN)_6]$ (1:1) containing 0.1 M KCl. (B) ECL-time curves of (a) g-C_3N_4/GCE, (b) MoS_2/g-C_3N_4/GCE, (c) TiO_2/MoS_2/g-C_3N_4/GCE, (d) 5hmC-PFc/TiO_2/MoS_2/g-C_3N_4/GCE, (e) TiO_2/MoS_2/g-C_3N_4/GCE incubated with PFc, (f) TiO_2/MoS_2/g-C_3N_4/GCE incubated with 5hmC in 10 mM PBS containing 100 mM $K_2S_2O_8$ (pH = 7.4).

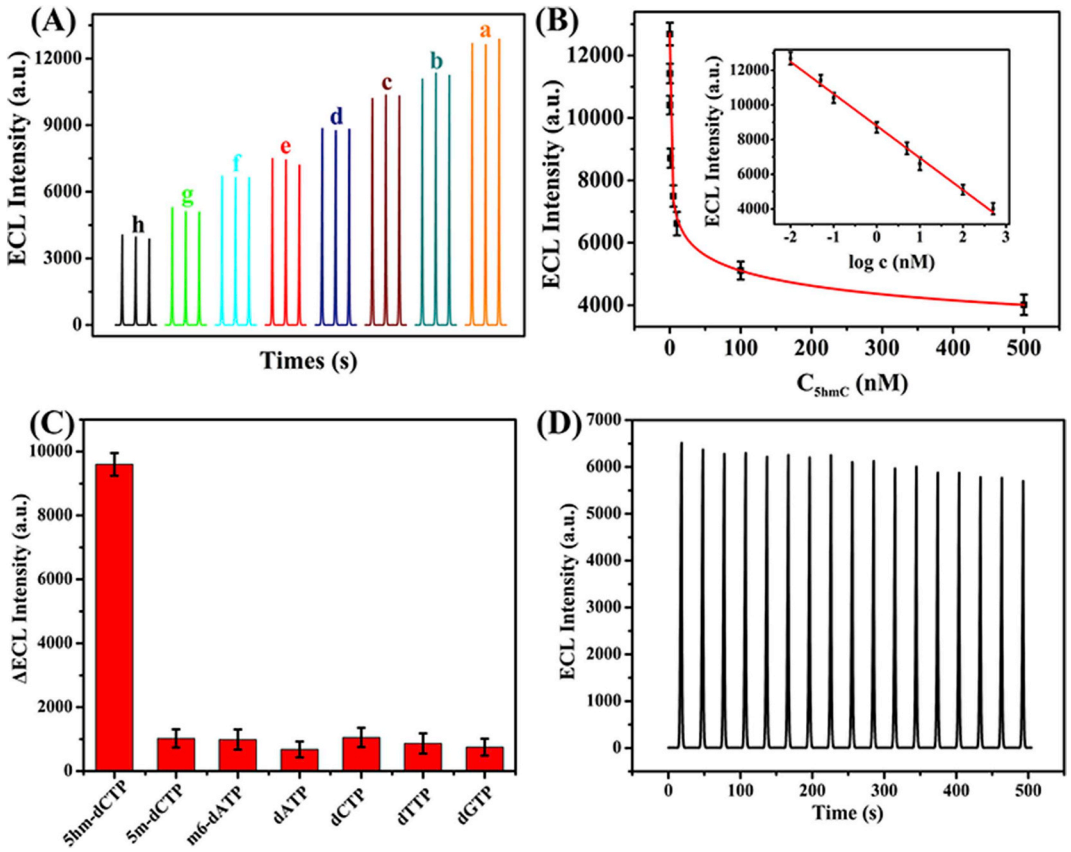

Fig. 3. (A) ECL intensity of the biosensor with different concentrations of 5hmC. a-i, 0.0100, 0.0500, 0.100, 1.00, 5.00, 10.0, 100, 500 nM. (B) The relationship between ECL intensity versus 5hmC concentration. (C) The ECL intensity change of the biosensor with different deoxyribonucleotides. (D) Continuous cyclic potential scans of the proposed ECL biosensor in 10 mM PBS containing 100 mM $K_2S_2O_8$ (pH = 7.4).

The specificity is an important part of the biosensor, thus, we conducted some experiments to investigate the specificity of the biosensor. To achieve this, 5m-dCTP, m6-ATP, dATP, dCTP, dTTP and dGTP were used as possible interferents. The ECL intensity changes ($\Delta ECL = ECL_1 - ECL_2$) of different targets were measured and compared, where ECL_1 represents the ECL intensity of the TiO_2/MoS_2/g-C_3N_4/GCE, ECL_2 represents the ECL intensity of TiO_2/MoS_2/g-C_3N_4/GCE incubated successively with different interferents, M. HhaI and PFc. As shown in Fig. 3C, the ΔECL of 5hmC is significantly higher than that of the interferents, which demonstrates the superior specificity of the developed method.

As one of the important performances of the biosensor, the stability was also assessed. As shown in Fig. 3D, the ECL intensity has no significant change with the 17 cycles and the relative standard deviation (RSD) is only 2.18%. Moreover, the ECL intensity is almost 91.0% when the biosensor was stored at 4 °C for 15 days. Thus, the biosensor has remarkable stability. The reproducibility of the biosensor was also investigated by detecting six 5hmC-PFc/TiO_2/MoS_2/g-C_3N_4/GCE at same condition. The ECL intensities of the six electrodes are almost same with the RSD was 2.98%, indicating the preeminent reproducibility of the biosensor.

Table 1
Performance comparison of the ECL biosensor with other methods for 5hmC detection.

Methods	Target	Linear range	Detection limit	Refs
Capillary electrophoresis	5hmC-DNA	0.09–90 nM	0.09 nM	[10]
Electrochemistry	5hm-dCTP	0.1–30 nM	32 pM	[56]
Electrochemistry	5hm-dCTP	0.5–90 nM	0.14 nM	[13]
Electrochemistry	5hmC-DNA	0.01–1000 pM	9.06 fM	[57]
Fluorescence	5hmC-DNA	0–100 nM	0.167 nM	[9]
Fluorescence	5hmC-DNA	0–150 nM	–	[58]
Photoelectrochemistry	5hm-dCTP	0.01–100 nM	3.4 pM	[59]
Photoelectrochemistry	5hm-dCTP	0.01–100 nM	4.12 pM	[12]
ECL	5hmC-DNA	0.5–100 pM	0.14 pM	[11]
ECL	5hmC-DNA	0.05–10 pM	12 fM	[60]
ECL	5hmC-DNA	0.05–10 nM	16.3 pM	[61]
ECL	5hmC-DNA	0.01–1000 pM	3.84 fM	[62]
ECL	5hm-dCTP	0.01–500 nM	3.21 pM	This work

3.5. Detection of 5hmC in samples

Many factors can influence the growth and yield of crops, such as heavy meal, salt, organic molecule, heat, chilling, etc [44–47]. Recently, as small organic molecule, antibiotic attracts more attentions due to the abuse of antibiotics in China, which leads to severe environmental problems. The antibiotics released into water and soil environment can be adsorbed by crops, and may influence plant physiological and biochemical processes. Thus, to prove the practical applicability of the developed method, the effect of different antibiotic to the 5hmC level in rice seedling was investigated. As shown in Fig. 4A–C, the 5hmC content in rice seedling roots, stems and leaves changed significantly by treating with different antibiotics (amoxicillin, tobramycin, chloramphenicol, roxithromycin, tetracycline, norfloxacin). In roots, only the 5hmC level of rice seedling roots treated by amoxicillin decreases, and the others increase. In stems, the 5hmC level of rice seedling stems decreases after treated with tetracycline, norfloxacin, and the others adversely increase. However, in the leaves, the 5hmC level of rice seedling leaves increases with treated by amoxicillin and tobramycin, and the others decreases. The results proved that antibiotics have an effect on the formation process of 5hmC [48–50]. This study may also provide new biomarkers and new methods for the evaluation of the ecotoxicological effects of antibiotics towards rice.

Marek's disease (MD) is one of the most deadly diseases for poultry, which was caused by the infected with MDV [51–53]. To decrease the economic losses, the early diagnosis for MD is necessary. For achieving it, suitable biomarker is essential. Thus, the effect of MDV on 5hmC content in genomic DNA of chicken fibroblasts cell was investigated. As seen in Fig. 4D–F, the 5hmC level decreases with the treatment of MDV. Further, the 5hmC level further decreases with the increase of the incubation time. The result demonstrated that 5hmC expression is closely related to viral infection [54,55]. This study may also provide an alternative biomarker for the detection of Marek's disease.

To prove the accuracy of the method, the detection results were compared with the ELISA method, and the relative error was less than 5.00%, indicating the higher accuracy of the biosensor.

4. Conclusions

In summary, a sensitive ECL biosensor was constructed for 5hmC detection based on the covalent bonding reaction between –SH of PFc and $–CH_2OH$ of 5hmC under the catalysis of M. HhaI, the ECL signal inhibition effect of PFc on g-C_3N_4. The biosensor shown excellent specificity and sensitivity for 5hmC detection with a low detection limit of 3.21 pM with the detection range of 0.01–500 nM. This biosensor was also used in the detection of 5hmC in genomic DNA of rice seedling after treatment with different antibiotics and in chicken embryo fibroblast cells after infection with MDV. The results indicated that the 5hmC level in rice seedling leaves increased with treated by amoxicillin and tobramycin, and decreased with treated by chloramphenicol, roxithromycin, tetracycline, norfloxacin. In addition, the expression level of 5hmC in chicken embryo fibroblast cell after infected with MDV was

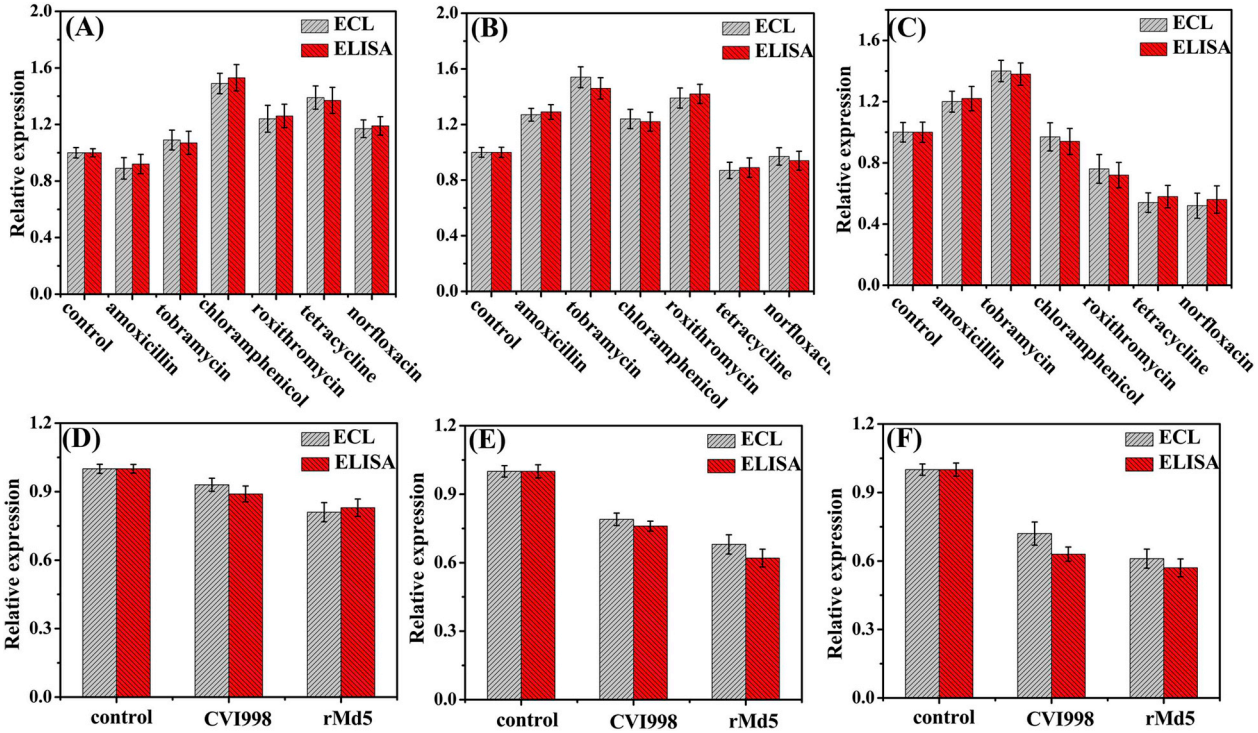

Fig. 4. Effect of different antibiotics on 5hmC expression in the genomic DNA of rice seedling roots (A), stems (B) and leaves (C). Effect of MDV (CVI998, RMD5) on 5hmC expression in the genomic DNA of chicken embryo fibroblast cell for 24 (D), 48 (E) and 72 h (F), respectively.

decreased. These results proved that the novel findings of this study may provide new biomarkers for the evaluation of ecotoxicological effects of antibiotics and in the detection of Marek's disease.

Credit author statement

Chengji Sui: Data curation, Formal analysis, Investigation, Methodology, Writing - original draft. Qian Wang: Data curation, Formal analysis, Investigation, Methodology, Writing - original draft. Yunlei Zhou: Resources, Data curation, Formal analysis, Funding acquisition, Investigation, Methodology, Validation, Project administration, Writing - review & editing. Dingding Zhang: Data curation, Investigation, Methodology. Huanshun Yin: Resources, Data curation, Formal analysis, Project administration, Validation, Supervision, Writing - review & editing. Shiyun Ai: Resources, Project administration, Validation, Supervision.

Declaration of competing interest

The authors declare that they have no known competing financial interests or personal relationships that could have appeared to influence the work reported in this paper.

Acknowledgments

This work was supported by the National Natural Science Foundation of China (21775090, 41807484), the Natural Science Foundation of Shandong Province of China (ZR2018MB028). All the authors thank prof. Sun for her kindly provision of chicken embryo fibroblast cell infected with and without MDV.

Appendix A. Supplementary data

Supplementary data to this article can be found online at https://doi.org/10.1016/j.talanta.2020.121211.

References

[1] G.R. Wyatt, S.S. Cohen, A new pyrimidine base from bacteriophage nucleic acids, Nature 170 (4338) (1952) 1072–1073.
[2] S. Kriaucionis, N. Heintz, The nuclear DNA base 5-hydroxymethylcytosine is present in purkinje neurons and the brain, Science 324 (5929) (2009) 929–930.
[3] M. Münzel, D. Globisch, T. Carell, 5-Hydroxymethylcytosine, the sixth base of the genome, Angew. Chem. Int. Ed. 50 (29) (2011) 6460–6468.
[4] S.-G. Jin, Y. Jiang, R. Qiu, T.A. Rauch, Y. Wang, G. Schackert, D. Krex, Q. Lu, G.P. Pfeifer, 5-Hydroxymethylcytosine is strongly depleted in human cancers but its levels do not correlate with IDH1 mutations, Canc. Res. 71 (24) (2011) 7360–7365.
[5] R. Yin, J. Mo, M. Lu, H. Wang, Detection of human urinary 5-hydroxymethylcytosine by stable isotope dilution HPLC-MS/MS analysis, Anal. Chem. 87 (3) (2015) 1846–1852.
[6] A. Khoshroo, L. Hosseinzadeh, A. Sobhani-Nasab, M. Rahimi-Nasrabadi, F. Ahmadi, Silver nanofibers/ionic liquid nanocomposite based electrochemical sensor for detection of clonazepam via electrochemically amplified detection, Microchem. J. 145 (2019) 1185–1190.
[7] R. Habibey, M. Ajami, S.A. Ebrahimi, A. Hesami, S. Babakoohi, H. Pazoki-Toroudi, Nitric oxide and renal protection in morphine-dependent rats, Free Radical Biol. Med. 49 (6) (2010) 1109–1118.
[8] M.R. Branco, G. Ficz, W. Reik, Uncovering the role of 5-hydroxymethylcytosine in the epigenome, Nat. Rev. Genet. 13 (2011) 7.
[9] H.-y. Chen, J.-R. Wei, J.-X. Pan, W. Zhang, F.-q. Dang, Z.-Q. Zhang, J. Zhang, Spectroscopic quantification of 5-hydroxymethylcytosine in genomic DNA using boric acid-functionalized nano-microsphere fluorescent probes, Biosens. Bioelectron. 91 (2017) 328–333.
[10] A.M. Krais, Y.J. Park, C. Plass, H.H. Schmeiser, Determination of genomic 5-hydroxymethyl-2′-deoxycytidine in human DNA by capillary electrophoresis with laser induced fluorescence, Epigenetics 6 (5) (2011) 560–565.
[11] S. Ma, H. Sun, Y. Li, H. Qi, J. Zheng, Discrimination between 5-hydroxymethylcytosine and 5-methylcytosine in DNA via selective electrogenerated chemiluminescence (ECL) labeling, Anal. Chem. 88 (20) (2016) 9934–9940.
[12] Y. Zhou, H. Yin, C. Sui, Y. Wang, S. Ai, Photoelectrochemical detection of 5-hydroxymethylcytosine in genomic DNA based on M. HhaI methyltransferase catalytic covalent bonding, Chem. Eng. J. 357 (2019) 94–102.
[13] H. Yin, Z. Yang, H. Wang, Y. Zhou, S. Ai, Electrochemical biosensor for hydroxymethylated DNA detection and β-glucosyltransferase activity assay based on enzymatic catalysis triggering signal amplification, Sensor. Actuator. B Chem. 243 (2017) 602–608.
[14] Y. Liu, P. Siejka-Zielińska, G. Velikova, Y. Bi, F. Yuan, M. Tomkova, C. Bai, L. Chen, B. Schuster-Böckler, C.-X. Song, Bisulfite-free direct detection of 5-methylcytosine and 5-hydroxymethylcytosine at base resolution, Nat. Biotechnol. 37 (4) (2019) 424–429.
[15] Z. Liu, W. Qi, G. Xu, Recent advances in electrochemiluminescence, Chem. Soc. Rev. 44 (10) (2015) 3117–3142.
[16] H. Sha, Y. Wang, Y. Zhang, H. Ke, X. Xiong, N. Jia, Enzyme-free ECL immunesensor based on PbS nanocrystals for highly sensitive detection of alpha fetoprotein, Sensor. Actuator. B Chem. 277 (2018) 157–163.
[17] Y. Zou, H. Zhang, Z. Wang, Q. Liu, Y. Liu, A novel ECL method for histone acetyltransferases (HATs) activity analysis by integrating HCR signal amplification and ECL silver clusters, Talanta 198 (2019) 39–44.
[18] D. Wang, Y. Li, Z. Lin, B. Qiu, L. Guo, Surface-enhanced electrochemiluminescence of Ru@SiO_2 for ultrasensitive detection of carcinoembryonic antigen, Anal. Chem. 87 (12) (2015) 5966–5972.
[19] Y.-B. Miao, H.-X. Ren, N. Gan, Y. Zhou, Y. Cao, T. Li, Y. Chen, A triple-amplification SPR electrochemiluminescence assay for chloramphenicol based on polymer enzyme-linked nanotracers and exonuclease-assisted target recycling, Biosens. Bioelectron. 86 (2016) 477–483.
[20] L. Jin, J. Qiao, J. Chen, N. Xu, M. Wu, Combination of area controllable sensing surface and bipolar electrode-electrochemiluminescence approach for the detection of tetracycline, Talanta 208 (2020) 120404.
[21] J. Lu, M. Yan, L. Ge, S. Ge, S. Wang, J. Yan, J. Yu, Electrochemiluminescence of blue-luminescent graphene quantum dots and its application in ultrasensitive aptasensor for adenosine triphosphate detection, Biosens. Bioelectron. 47 (2013) 271–277.
[22] Y. Wu, J. Yang, Z. Zheng, Z. Li, F. Lu, Y. Chen, W. Gao, Three-dimensional Tri-SNSs-layered electrodeposited reduced graphene oxide for ECL biosensing of DNA, Talanta 188 (2018) 58–65.
[23] M. Wang, Y. Zhou, H. Yin, W. Jiang, H. Wang, S. Ai, Signal-on electrochemiluminescence biosensor for microRNA-319a detection based on two-stage isothermal strand-displacement polymerase reaction, Biosens. Bioelectron. 107 (2018) 34–39.
[24] Q. Feng, M. Wang, X. Zhao, P. Wang, Construction of a cytosine-adjusted electrochemiluminescence resonance energy transfer system for microRNA detection, Langmuir 34 (34) (2018) 10153–10162.
[25] W. Jiang, L. Wu, J. Duan, H. Yin, S. Ai, Ultrasensitive electrochemiluminescence immunosensor for 5-hydroxymethylcytosine detection based on Fe_3O_4@SiO_2 nanoparticles and PAMAM dendrimers, Biosens. Bioelectron. 99 (2018) 660–666.
[26] W. Jiang, H. Yin, Y. Zhou, J. Duan, H. Li, M. Wang, G.I.N. Waterhouse, S. Ai, A novel electrochemiluminescence biosensor for the detection of 5-methylcytosine, TET 1 protein and β-glucosyltransferase activities based on gold nanoclusters-H_2O_2 system, Sensor. Actuator. B Chem. 274 (2018) 144–151.
[27] D. Long, Y. Shang, Y. Qiu, B. Zhou, P. Yang, A single-cell analysis platform for electrochemiluminescent detection of platelets adhesion to endothelial cells based on Au@DL-ZnCQDs nanoprobes, Biosens. Bioelectron. 102 (2018) 553–559.
[28] Y.-Z. Wang, N. Hao, Q.-M. Feng, H.-W. Shi, J.-J. Xu, H.-Y. Chen, A ratiometric electrochemiluminescence detection for cancer cells using g-C_3N_4 nanosheets and Ag–PAMAM–luminol nanocomposites, Biosens. Bioelectron. 77 (2016) 76–82.
[29] S. Chen, Y. Dou, Z. Zhao, F. Li, J. Su, C. Fan, S. Song, High-sensitivity and high-efficiency detection of DNA hydroxymethylation in genomic DNA by multiplexing electrochemical biosensing, Anal. Chem. 88 (7) (2016) 3476–3480.
[30] Z. Liutkevičiūtė, E. Kriukienė, I. Grigaitytė, V. Masevičius, S. Klimašauskas, Methyltransferase-directed derivatization of 5-hydroxymethylcytosine in DNA, Angew. Chem. Int. Ed. 50 (9) (2011) 2090–2093.
[31] J. Chang, X. Wang, J. Wang, H. Li, F. Li, Nucleic acid-functionalized metal–organic framework-based homogeneous electrochemical biosensor for simultaneous detection of multiple tumor biomarkers, Anal. Chem. 91 (5) (2019) 3604–3610.
[32] P. Gai, C. Gu, H. Li, X. Sun, F. Li, Ultrasensitive ratiometric homogeneous electrochemical microRNA biosensing via target-triggered Ru(III) release and redox recycling, Anal. Chem. 89 (22) (2017) 12293–12298.
[33] X. Li, L. Zhu, Y. Zhou, H. Yin, S. Ai, Enhanced photoelectrochemical method for sensitive detection of protein kinase A activity using TiO_2/g-C_3N_4, PAMAM dendrimer, and alkaline phosphatase, Anal. Chem. 89 (4) (2017) 2369–2376.
[34] K. Ai, C. Ruan, M. Shen, L. Lu, MoS_2 nanosheets with widened interlayer spacing for high-efficiency removal of mercury in aquatic systems, Adv. Funct. Mater. 26 (30) (2016) 5542–5549.
[35] Y. Deng, M. Xing, J. Zhang, An advanced TiO_2/Fe_2TiO_5/Fe_2O_3 triple-heterojunction with enhanced and stable visible-light-driven fenton reaction for the removal of organic pollutants, Appl. Catal. B Environ. 211 (2017) 157–166.
[36] B. Zhang, B. Liu, G. Chen, D. Tang, Redox and catalysis 'all-in-one' infinite coordination polymer for electrochemical immunosensor of tumor markers, Biosens. Bioelectron. 64 (2015) 6–12.
[37] X. Hua, D. Tian, F. Xia, C. Zhou, G. Wu, Ultrasensitive electrochemiluminescent immunosensor using MoS_2/g-C_3N_4 nanosheets, J. Electrochem. Soc. 164 (9) (2017) B456–B462.
[38] X. Ou, C. Fang, Y. Fan, H. Chen, S. Chen, S. Wei, Sandwich-configuration electrochemiluminescence biosensor based on Ag nanocubes–polyamidoamine dendrimer–luminol nanocomposite for Con A detection, Sensor. Actuator. B Chem. 228 (2016) 625–633.
[39] S.-K. Li, Z.-T. Liu, J.-Y. Li, A.-Y. Chen, Y.-Q. Chai, R. Yuan, Y. Zhuo, Enzyme-free target recycling and double-output amplification system for electrochemiluminescent assay of Mucin 1 with MoS_2 nanoflowers as co-reaction accelerator, ACS Appl. Mater. Interfaces 10 (17) (2018) 14483–14490.

[40] T. Hou, W. Li, X. Liu, F. Li, Label-free and enzyme-free homogeneous electrochemical biosensing strategy based on hybridization chain reaction: a facile, sensitive, and highly specific microRNA assay, Anal. Chem. 87 (22) (2015) 11368–11374.
[41] G. Zhu, P. Gai, Y. Yang, X. Zhang, J. Chen, Electrochemical sensor for naphthols based on gold nanoparticles/hollow nitrogen-doped carbon microsphere hybrids functionalized with SH-β-cyclodextrin, Anal. Chim. Acta 723 (2012) 33–38.
[42] X. Liu, P. Liu, Y. Tang, L. Yang, L. Li, Z. Qi, D. Li, D.K.Y. Wong, A photoelectrochemical aptasensor based on a 3D flower-like TiO_2-MoS_2-gold nanoparticle heterostructure for detection of kanamycin, Biosens. Bioelectron. 112 (2018) 193–201.
[43] Q.-M. Feng, Y.-H. Guo, J.-J. Xu, H.-Y. Chen, A surface-confined DNA assembly amplification strategy on DNA nanostructural scaffold for electrochemiluminescence biosensing, Biosens. Bioelectron. 100 (2018) 571–576.
[44] W.Y. Song, S.P. Peng, C.Y. Shao, H.B. Shao, H.C. Yang, Ethylene glycol tetra-acetic acid and salicylic acid improve anti-oxidative ability of maize seedling leaves under heavy-metal and polyethylene glycol 6000-simulated drought stress, Plant Biosyst. Int. J. Dealing All Aspects Plant Biol. 148 (1) (2014) 96–108.
[45] M. Zhang, G.-Q. Zhang, H.-H. Kang, S.-M. Zhou, W. Wang, TaPUB1, a putative E3 Ligase gene from wheat, enhances salt stress tolerance in transgenic nicotiana benthamiana, Plant Cell Physiol. 58 (10) (2017) 1673–1688.
[46] J. Li, Y. Wang, B. Yu, Q. Song, Y. Liu, T.H.H. Chen, G. Li, X. Yang, Ectopic expression of StCBF1and ScCBF1 have different functions in response to freezing and drought stresses in Arabidopsis, Plant Sci. 270 (2018) 221–233.
[47] G. Wang, F. Kong, S. Zhang, X. Meng, Y. Wang, Q. Meng, A tomato chloroplast-targeted DnaJ protein protects Rubisco activity under heat stress, J. Exp. Bot. 66 (11) (2015) 3027–3040.
[48] P. Moricova, V. Ondrej, B. Navratilova, L. Luhova, Changes of DNA methylation and hydroxymethylation in plant protoplast cultures, Acta Biochim. Pol. 60 (1) (2013) 33–36.
[49] S. Kumar, Epigenomics of plant responses to environmental stress, Epigenomes 2 (1) (2018) 6.
[50] Y. Tang, J. Xiong, H.-P. Jiang, S.-J. Zheng, Y.-Q. Feng, B.-F. Yuan, Determination of oxidation products of 5-methylcytosine in plants by chemical derivatization coupled with liquid chromatography/tandem mass spectrometry Analysis, Anal. Chem. 86 (15) (2014) 7764–7772.
[51] S. Yang, L. Wang, S. Sun, Natural infection with avian Hepatitis E virus and Marek's disease virus in brown layer chickens in China, Avian Dis. 60 (3) (2016) 698–704.
[52] D. Wang, S. Sun, M. Heidari, Marek's disease vaccine activates chicken macrophages, J. Vet. Sci. 19 (3) (2018) 375–383.
[53] N. Cui, S. Su, P. Sun, Y. Zhang, N. Han, Z. Cui, Isolation and pathogenic analysis of virulent Marek's disease virus field strain in China, Poultry Sci. 95 (7) (2016) 1521–1528.
[54] F. Tian, F. Zhan, N.D. VanderKraats, J.F. Hiken, J.R. Edwards, H. Zhang, K. Zhao, J. Song, DNMT gene expression and methylome in Marek's disease resistant and susceptible chickens prior to and following infection by MDV, Epigenetics 8 (4) (2013) 431–444.
[55] S. Pejaković, B. Muylkens, DNA Methylation and Hydroxymethylation on the Viral Telomerase RNA Subunit Promoter in a Model of Herpesvirus Induced Oncogenesis, (2017).
[56] Z. Yang, W. Jiang, F. Liu, Y. Zhou, H. Yin, S. Ai, A novel electrochemical immunosensor for the quantitative detection of 5-hydroxymethylcytosine in genomic DNA of breast cancer tissue, Chem. Commun. 51 (78) (2015) 14671–14673.
[57] L. Cui, J. Hu, M. Wang, C.-c. Li, C.-y. Zhang, Label-free and immobilization-free electrochemical magnetobiosensor for sensitive detection of 5-hydroxymethylcytosine in genomic DNA, Anal. Chem. 91 (2) (2019) 1232–1236.
[58] T. Hong, T. Wang, P. Guo, X. Xing, F. Ding, Y. Chen, J. Wu, J. Ma, F. Wu, X. Zhou, Fluorescent strategy based on cationic conjugated polymer fluorescence resonance energy transfer for the quantification of 5-(hydroxymethyl)cytosine in genomic DNA, Anal. Chem. 85 (22) (2013) 10797–10802.
[59] C. Sui, T. Wang, Y. Zhou, H. Yin, X. Meng, S. Zhang, G.I.N. Waterhouse, Q. Xu, Y. Zhuge, S. Ai, Photoelectrochemical biosensor for hydroxymethylated DNA detection and T4-β-glucosyltransferase activity assay based on WS_2 nanosheets and carbon dots, Biosens. Bioelectron. 127 (2019) 38–44.
[60] H. Sun, H. Wang, W. Bai, L. Bao, J. Lin, Y. Li, Sensitive electrogenerated chemiluminescence biosensing method for the determination of DNA hydroxymethylation based on $Ru(bpy)^{32+}$-doped silica nanoparticles labeling and MoS_2-poly(acrylic acid) nanosheets modified electrode, Talanta 191 (2019) 350–356.
[61] Y. Zhang, Y. Li, Y. Wei, H. Sun, H. Wang, A sensitive signal-off electrogenerated chemiluminescence biosensing method for the discrimination of DNA hydroxymethylation based on glycosylation modification and signal quenching from ferroceneboronic acid, Talanta 170 (2017) 546–551.
[62] Y. Wei, H. Sun, J. Li, Y. Zhang, Y. Li, J. Lin, T. Wang, M. Zhou, Electrogenerated chemiluminescence biosensing method for highly sensitive detection of DNA hydroxymethylation: combining glycosylation with $Ru(phen)^{32+}$-assembled graphene oxide, J. Electroanal. Chem. 795 (2017) 123–129.